Specific Heat of a Quantum Critical Metal

Ori Grossman,* Johannes S. Hofmann, Tobias Holder, and Erez Berg†
Department of Condensed Matter Physics, Weizmann Institute of Science, Rehovot 76100, Israel

(Received 21 October 2020; accepted 30 May 2021; published 30 June 2021)

We investigate the specific heat c, near an Ising nematic quantum critical point (QCP), using sign problem-free quantum Monte Carlo simulations. Cooling towards the QCP, we find a broad regime of temperature where c/T is close to the value expected from the noninteracting band structure, even for a moderately large coupling strength. At lower temperature, we observe a rapid rise of c/T, followed by a drop to zero as the system becomes superconducting. The spin susceptibility begins to drop at roughly the same temperature where the enhancement of c/T onsets, most likely due to the opening of a gap associated with superconducting fluctuations. These findings suggest that superconductivity and non-Fermi liquid behavior (manifested in an enhancement of the effective mass) onset at comparable energy scales. We support these conclusions with an analytical perturbative calculation.

DOI: 10.1103/PhysRevLett.127.017601

Introduction.—Understanding the continuous formation of order in a Fermi liquid remains a central challenge in the study of strongly correlated electron systems. This problem is complicated by the presence of the gapless quasiparticles at the Fermi surface, which makes the canonical Landau-Ginzburg-Wilson approach of quantum criticality inapplicable [1–8]. Pinning down the nature of metallic quantum critical points (QCPs) in the case of two spatial dimensions (which is relevant to many quantum materials) has proven particularly challenging [9–26].

The metallic state in the vicinity of the QCP may follow one of two distinct scenarios [22,29,30]. In the first scenario, a non-Fermi liquid (NFL) metal emerges near the QCP, where electronic quasiparticles become strongly incoherent due to their strong scattering off the critical fluctuations of the order parameter. In the second scenario, superconductivity mediated by the same critical fluctuations gaps the Fermi surface before the non-Fermi liquid develops, and as a result the normal state in the quantum critical regime is a Fermi liquidlike state with coherent quasiparticles. A successful description of the critical metal has to take into consideration these two competing effects on the same footing. The resulting multichannel strong coupling problem is currently not amenable to a controlled analytical approach.

A salient feature expected for a nearly-critical Fermi liquid, along with the enhancement of quasiparticle scattering, is a divergence of the effective mass, m^* [3]. Such a divergence can be probed either by measuring the specific heat coefficient at low temperatures, $c/T \propto m^*$ [31–34], or by other means, such as by measurements of de Haas–van Alphen oscillations [35,36]. For example, in the case where the quantum critical fluctuations carry near-zero momentum, a power law divergence of the specific heat is expected; within the random phase approximation (RPA), $c/T \sim T^{-1/3}$ [37]. However, the divergence of c/T may be preempted by a transition to a superconductor. The main question addressed in this work is whether the quantum critical regime above the superconducting T_c is characterized by a pronounced enhancement of c/T upon approaching the QCP.

In recent years, it has been demonstrated that models for quantum critical metals can be efficiently simulated using the numerically exact determinant quantum Monte Carlo (DQMC) method without suffering from the notorious fermion sign problem [38–50]. Here, we report the first DQMC results for the specific heat of a metallic Ising-nematic QCP at which a discrete C_4 rotation symmetry is spontaneously broken.

Previous works on this model focused on the self-energy and transport properties, finding signatures of the breakdown of Fermi liquid behavior, in an extended temperature window above the superconducting critical temperature T_c near the QCP [51]. Interestingly, we find that the specific heat in the same temperature regime is close to the noninteracting value down to a temperature $\sim 2T_c$, which we identify as the onset of superconducting fluctuations, probed by the opening of a spin gap. Thus, the specific heat does not exhibit a broad non-Fermi liquid regime near the QCP. Inspired by the perturbative structure of the theory, we propose a resolution to this apparent discrepancy between the transport and thermodynamic properties.

Model and method.—The model is defined on a two-dimensional square lattice with a single (spinful) fermionic state per lattice site and a pseudospin 1/2 boson on each nearest-neighbor bond [Fig. 1(a)] [40]. The system is described by the Hamiltonian $H = H_f + H_b + H_{\text{int}}$ with

 © 2021 American Physical Society

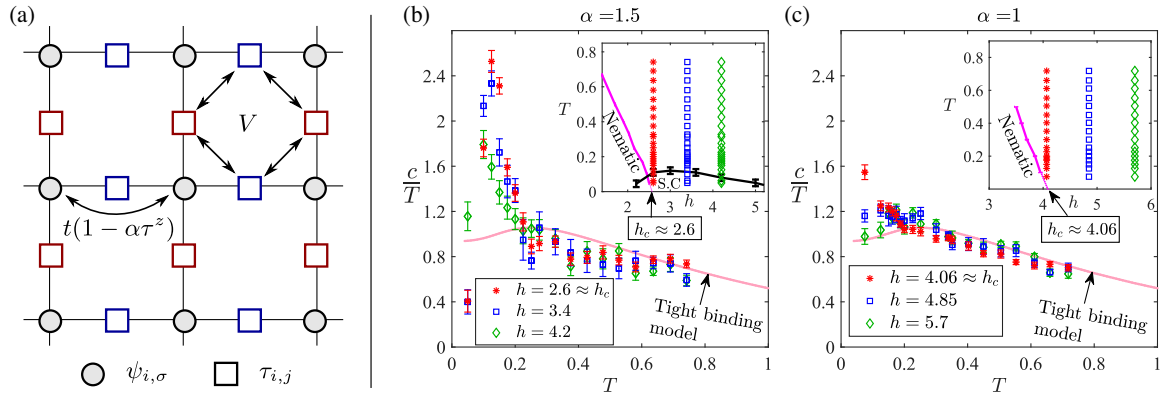

FIG. 1. (a) Visualization of the model Hamiltonian. (b),(c) c/T as a function of temperature at various h values, for different coupling constants: (b) $\alpha = 1.5$, $V = 0.5$, and (c) $\alpha = 1$, $V = 1$. In both cases, $\mu = -1$ and $L = 12$. The solid line is c/T of the noninteracting tight binding model. The inset shows the phase diagram in the (h, T) plane. For $\alpha = 1.5$, the black line shows the superconducting T_c vs h. For $\alpha = 1$, we estimate $T_c \lesssim 0.02$ at $h \approx h_c$.

$$
\begin{aligned}
H_f &= -t\sum_{\langle i,j\rangle,\sigma} \psi^\dagger_{i,\sigma}\psi_{j,\sigma} - \mu\sum_{i,\sigma}\psi^\dagger_{i,\sigma}\psi_{i,\sigma},\\
H_b &= V\sum_{\langle\langle i,j\rangle;\langle k,l\rangle\rangle} \tau^z_{i,j}\tau^z_{k,l} - h\sum_{\langle i,j\rangle}\tau^x_{i,j},\\
H_{\text{int}} &= \alpha t\sum_{\langle i,j\rangle,\sigma} \tau^z_{i,j}\psi^\dagger_{i,\sigma}\psi_{j,\sigma}.
\end{aligned}
\tag{1}
$$

Here, $\psi^\dagger_{i,\sigma}$ creates a fermion on site i of spin $\sigma = \downarrow, \uparrow$, $\langle i, j\rangle$ denote nearest-neighbor bonds, and t, μ are the hopping amplitude and chemical potential, respectively. The pseudospins, represented by the Pauli matrices $\tau^{\alpha=x,y,z}_{i,j}$, are governed by a transverse field Ising model. The interaction strength between spins on nearest-neighbor bonds $\langle\langle i, j\rangle; \langle k, l\rangle\rangle$ is given by $V > 0$, h sets the transverse field strength, and α is the dimensionless coupling strength between the pseudospins and the fermions. Physically, the pseudospins can originate from a purely electronic interaction via Hubbard-Stratonovich transformation, or from bosonic degrees of freedom such as phonons. More importantly, the model is designed to host an Ising nematic critical point, which separates an ordered phase, where the C_4 rotational symmetry of the lattice is spontaneously broken, from a C_4 symmetric phase. In the ordered phase, the expectation value of τ^z on horizontal bonds becomes different from that of τ^z on vertical bonds, breaking the 90° rotational symmetry of the lattice. The transition can be tuned by the transverse field h, and remains continuous down to low temperature [40,51].

We use the ALF package [52], a general implementation of the auxiliary field quantum Monte Carlo algorithm [53,54], to solve the Hamiltonian from above. The negative-sign problem is absent due to time-reversal symmetry for each space-time configuration of $\tau^z_{i,j}$. Global updates of the boson fields, that are constructed according to the Wolf algorithm [55], are used to shorten both the autocorrelation and thermalization times. An artificial orbital magnetic field that couples oppositely to spin up and spin down electrons, corresponding to one flux quantum in the entire system, is applied to reduce finite size effects [40,56]. For more details of the QMC implementation, see Refs. [40,57]. The specific heat c may be evaluated from (i) the numerical derivative of the energy, $c = d\langle H\rangle/dT$, or (ii) the fluctuations of the energy, $c = \beta^2(\langle H^2\rangle - \langle H\rangle^2)$, where $\beta = 1/T$ [62]. In our model, we found that approach (i) converges much faster than (ii) [57].

In the following, we focus on two parameter sets, $(\alpha = 1.5, V/t = 0.5)$ and $(\alpha = 1, V/t = 1)$. The chemical potential is fixed to $\mu/t = -1$. We point out that there is a van Hove singularity in the band dispersion at $\mu = 0$. In the Supplemental Material [57] we present results for $\alpha = 1, \mu/t = -0.5$, where effects of the proximity to the van Hove singularity are more pronounced. We use t as the unit of energy in the remainder.

Results.—We begin by reviewing the phase diagram for the model of Eq. (1), described in Refs. [40,51]. To locate the nematic phase transition, we examine the nematic susceptibility

$$
\chi(h, T) = \frac{1}{L^2}\sum_{i,j}\int_0^\beta d\tau\langle N_i(\tau)N_j(0)\rangle, \tag{2}
$$

with the nematic order parameter $N_i = \sum_j \zeta_{ij}\tau^z_{ij}$, where $\zeta_{ij} = 1/4$ for $\mathbf{r}_{ij} = \pm\hat{\mathbf{x}}$ [blue squares in Fig. 1(a)], $\zeta_{ij} = -1/4$ for $\mathbf{r}_{ij} = \pm\hat{\mathbf{y}}$ [red squares in Fig. 1(a)], and $\zeta_{ij} = 0$ otherwise. L is the linear system size. We present the inverse susceptibility as a function of temperature in Fig. 2 for three transverse field values h and two coupling strengths α. The nematic fluctuations are enhanced as the temperature is reduced. χ^{-1} saturates for the larger values of h, which indicates a nematic-disordered ground state, while the susceptibility nearly diverges $(\chi^{-1} \to 0)$ for the lowest transverse field strength signalling a nematically ordered phase. The critical transverse field

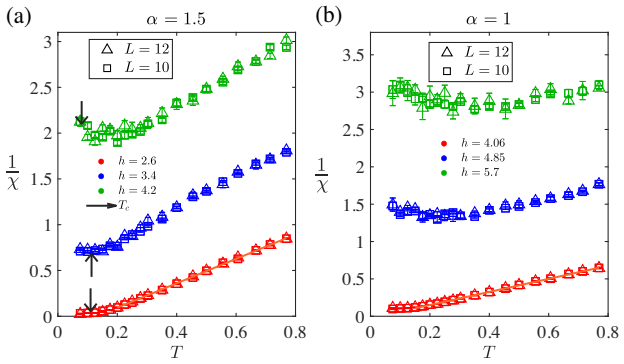

FIG. 2. The inverse nematic susceptibility $(1/\chi)$ as a function of temperature, for two different system sizes ($L = 10$, 12). In (a) for $\alpha = 1.5$ and in (b) for $\alpha = 1$. The linear behavior of $1/\chi$ as a function of T (orange), at $h \approx h_c$, is extended to lower temperatures for $\alpha = 1$. This can be a consequence of the lower T_c at $\alpha = 1$, and therefore the fermions are gapped out at lower temperatures. The arrows (black) indicate the superconducting T_c obtained from Ref. [51] for $\alpha = 1.5$.

$h_c(T)$ at a given temperature T is determined by a finite size scaling analysis, assuming classical 2D Ising critical exponents [57], and the resulting phase diagram is shown in the inset of Fig. 1 for the two different values of α. The quantum critical point is located at $h_c = \lim_{T\to 0} h_c(T)$. The superconducting transition temperature T_c, extracted from a scaling analysis of the s-wave pairing susceptibility [57], also appears in the insets of Fig. 1 for $\alpha = 1.5$. For $\alpha = 1$, the maximal T_c is smaller than 0.025 [57] and is not shown.

We now turn to the specific heat $c(T)$ at and away from the QCP. Figures 1(b), 1(c) show c/T for $\alpha = 1.5$, 1 respectively. At high temperatures, c/T is close to the value computed from the noninteracting tight-binding model (solid line) [63]. The broad maximum in the tight-binding curve at $T \approx 0.25$ is due to the van Hove singularity in the band structure. In the stronger coupling case ($\alpha = 1.5$), a pronounced peak appears in c/T at low temperatures. At $h = 2.6 \approx h_c$, the peak position occurs at $T_{\text{peak}} = 0.12 \pm 0.02$, which is slightly above the superconducting transition at $T_c = 0.1 \pm 0.02$. We note that, since the superconducting transition is of the Berezinskii-Kosterlitz-Thouless type, the singularity of c at T_c should be very weak, and hence T_{peak} is not generally expected to coincide with T_c. Upon increasing h, the peak shifts to a lower temperature.

At the weaker coupling strength ($\alpha = 1$), such a clear peak is absent. At the lowest temperatures, there is an enhancement of the specific heat relative to the tight-binding model. This enhancement is most pronounced near the QCP. It is likely that c/T drops to zero at even lower temperatures, resulting in a finite-T peak in c/T, as in the $\alpha = 1.5$ case.

An enhancement in c/T may originate either from an opening of a gap in the quasiparticle spectrum or from an increase of the quasiparticle effective mass [64]. Evidently, for $\alpha = 1.5$, the peak in c/T [Fig. 1(b)] appears both near the QCP and away from it, hence is likely not caused by an enhanced m^* due to quantum critical fluctuations. The shift of the peak position upon increasing h mirrors the decrease of the superconducting critical temperature, suggesting that the superconducting gap opening is the main source of the peak in c/T. The situation is less clear for the weaker coupling $\alpha = 1$ [Fig. 1(c)], where a significant enhancement of c/T is only detectable near $h = h_c$.

In order to identify the origin of the low-temperature enhancement of the specific heat, we study the spin susceptibility,

$$\chi_{S^z} = \frac{1}{L^2}\sum_{i,j}\int_0^\beta d\tau \langle \hat{S}_i^z(\tau)\hat{S}_j^z(0)\rangle, \tag{3}$$

where $\hat{S}_i^z = \frac{1}{2}(\psi_{i,\uparrow}^\dagger \psi_{i,\uparrow} - \psi_{i,\downarrow}^\dagger \psi_{i,\downarrow})$. χ_{S^z} is shown in Fig. 3. The spin susceptibility is roughly constant for $T > 0.2$ ($T > 0.1$) for $\alpha = 1.5$ ($\alpha = 1$). As the temperature is lowered further, χ_{S^z} begins dropping dramatically, consistent with the opening of a spin gap.

The temperature where the suppression of χ_{S^z} onsets is comparable to the temperature at which c/T begins to rise (Fig. 1). This leads to an interpretation of both the enhancement of c/T and the suppression of χ_{S^z} as a signature of an opening of a gap, most likely associated with superconducting fluctuations. Further evidence for this interpretation is provided by a rapid growth of the superconducting susceptibility and a suppression of the single-particle density of states near the Fermi level, which both onset at a similar temperature [57]. Note that this implies that the gap at $h \approx h_c$ onset at a temperature significantly larger than the superconducting critical temperature, $T_c \approx 0.1$ for $\alpha = 1.5$ (marked by black arrows in Fig. 3(a), and $T_c \lesssim 0.02$ for $\alpha = 1$ [57]. Such a regime is commonly referred to as a "pseudogap regime" (or a regime of "preformed Cooper pairs" without long-range phase

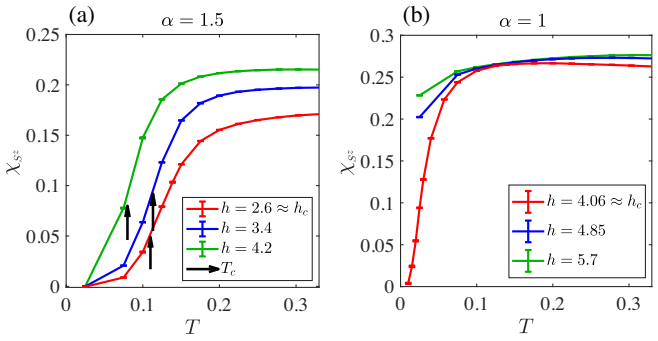

FIG. 3. The spin susceptibility χ_{S^z} as a function of temperature at various h values for the two different coupling constants. In (a) for $\alpha = 1.5$ and in (b) for $\alpha = 1$. As before, the arrows (black) indicate the superconducting T_c obtained from Ref. [51] for $\alpha = 1.5$. The system size is $L = 12$.

coherence). This behavior is in contrast to the expectation from weak-coupling mean-field theory, which predicts a gap that onsets concomitantly with T_c, but is in agreement with prior QMC results in models of quantum critical metals at intermediate to strong coupling [39,51].

The temperature range where χ_{S^z} is approximately constant, above the onset of the spin gap, can be interpreted in terms of a Fermi liquid. This interpretation is supported by the fact that, in the same regime, c/T is not strongly temperature dependent, as shown in Fig. 1 (and its temperature dependence can mostly be ascribed to band structure effects). In addition, the single-particle density of states at the Fermi level is found to be weakly temperature dependent in the same regime [57]. Within Fermi liquid theory, $c/T \propto m^*$, the single-particle density of states is proportional to Zm^*, where Z is the quasiparticle weight [65], and $\chi_{S^z} = \pi^{-2}(1+F_0^a)^{-1}k_F m^*$. Here, F_0^a is the isotropic, spin-antisymmetric component of the Landau quasiparticle interaction. Hence, at temperature above the onset of a spin gap, we can explain our data qualitatively by assuming that for $\alpha = 1$, $Z \approx 1$ and F_0^a is small. For $\alpha = 1.5$, in contrast, Z decreases substantially and F_0^a grows as h approaches h_c.

Combining the above arguments suggests the following picture for the behavior at $h \approx h_c$: (i) In a broad temperature range below the Fermi energy E_F, the system's thermodynamic properties are roughly consistent with Landau's Fermi liquid theory. (ii) Below a certain temperature, smaller than E_F but significantly larger than the superconducting T_c, c/T is enhanced, more or less concomitantly with a suppression of the spin susceptibility and the single-particle density of states. All these effects are most probably due to the onset of a gap due to superconducting fluctuations. (iii) At the lowest temperatures (below T_c) superconductivity is established.

Perturbation theory.—It is useful to relate our findings at strong coupling with the results of the standard RPA analysis [37]. The perturbative calculation is controlled in the limit of a large number N of fermion species (the physical value is $N = 2$) and not too low temperatures, as discussed below. For simplicity, we consider a system with dispersion $\varepsilon(\boldsymbol{k}) = \frac{\boldsymbol{k}^2}{2m} - \mu$. The four-fermion interaction is taken to be of the form

$$U(\boldsymbol{q},\boldsymbol{k},\boldsymbol{k}') = \frac{g^2 f_{\boldsymbol{k}-\boldsymbol{q}/2} f_{\boldsymbol{k}'+\boldsymbol{q}/2}}{N(r_0 + |\boldsymbol{q}|^2)}, \tag{4}$$

where $\boldsymbol{q}$ is the momentum transfer, g^2 is the coupling strength, and $f_{\boldsymbol{k}}$ is the nematic form factor: $f_{\boldsymbol{k}} = \cos k_x - \cos k_y$. The parameter r_0 is used to tune the system to the QCP, which occurs at $r_0 = r_c > 0$.

At $r_0 = r_c$, the specific heat is given by [57]

$$c(T) = \frac{\pi}{6} mNT\left[1 + \frac{A}{N}\left(\frac{g^4}{E_F T}\right)^{\frac{1}{3}} + O\left(\frac{1}{N^2}\right)\right], \tag{5}$$

where $A \approx 0.19$. The second term in the square brackets in Eq. (5) describes the enhancement of the specific heat due to quantum critical fluctuations. This term becomes significant compared to the first (noninteracting) term at a temperature $T_{\mathrm{NFL}} \propto g^4/N^3 E_F$. T_{NFL} is the temperature below which electrons lose their coherence, and the Fermi liquid description breaks down. At the same temperature, terms which are naively of higher order in $1/N$ become parametrically enhanced, and the $1/N$ expansion is no longer controlled [16,17,66]. Moreover, solving the linearized Eliashberg equation for the pairing vertex gives that $T_c \propto T_{\mathrm{NFL}}$ [57,67]. Thus, the weak coupling analysis predicts no parametric separation in temperature between the breakdown of Fermi liquid theory (manifested as a divergence of c/T) and the onset of a pairing gap. This conclusion is corroborated by an RPA analysis of a lattice model including the full tight-binding dispersion [Eq. (1)], showing no significant deviation of c/T relative to the noninteracting value for $T \gtrsim 0.2$ [57]. These observations mirror the picture that emerges at moderate to strong coupling from our QMC results, i.e., the enhancement of c/T, relative to the value expected from the band structure, onsets at the same temperature where a pairing gap appears.

Discussion.—In this work, we have examined the specific heat in the vicinity of a quantum critical point in a metal, using unbiased, numerically exact QMC simulations. We find that, upon cooling the system towards the quantum critical point, c/T is enhanced relative to the band structure value. The enhancement of c/T onsets at roughly the same temperature where the spin susceptibility and the single-particle density of states exhibit a downturn, signaling the appearance of a gap, most likely due to the onset of superconducting fluctuations. c/T is suppressed sharply upon entering the superconducting phase that covers the QCP.

Thus, our main conclusion is that within our model, there is no broad non-Fermi liquid regime characterized by a diverging c/T near the QCP. This is most probably because the quantum critical enhancement of c/T is preempted by the opening of a pairing gap. These observations are qualitatively consistent with the expectation from the weak-coupling RPA analysis, which predicts that T_{NFL} and T_c are of the same order of magnitude. However, in our simulations (performed in moderate to strong coupling) we find that the gap due to superconducting fluctuations appears at a temperature significantly above T_c, in contrast to the weak-coupling analysis in which the superconducting transition is essentially mean-field-like.

Above the gap opening temperature, we find a broad temperature regime where c/T shows no significant enhancement relative to the band structure value. This is surprising, since in this model, the same temperature regime has been shown to exhibit strong deviations from Fermi liquid theory in the frequency dependence of the self-energy and the temperature dependence of the

transport scattering rate [51,68]. This apparent discrepancy can be understood from the fact that, in this regime, the quasiparticles are still coherent [in the sense that their self-energy $\Sigma(i\omega_n)$ is smaller than ω_n, even at the smallest Matsubara frequency [57]], and the effective mass is not significantly enhanced. However, the self-energy (and hence the scattering rate) has a non-Fermi liquid temperature dependence [69–71].

We end with two comments regarding the implications of our study for experiments in quantum materials. First, our results imply that observing a divergence of m^* near a QCP generally requires suppressing superconductivity, e.g., by applying a magnetic field (which is unfortunately impossible in our simulations without introducing a fermion sign problem). Second, it is interesting to note that in $FeSe_{1-x}S_x$, a broad regime of quasilinear resistivity is observed near the putative nematic QCP [72–74] with no accompanying discernible enhancement of m^* [75]. These findings may be explained by the presence of coherent quasiparticles scattered by quantum critical fluctuations, analogous to the behavior found in our model.

The auxillary field QMC simulations were carried out using the ALF package [76].

We thank A. Chubukov, S. Kivelson, and Y. Schattner for useful discussions. This work was supported by the European Research Council (ERC) under grant HQMAT (Grant Agreement No. 817799), the US-Israel Binational Science Foundation (BSF) under Grant No. 2018217, the Minerva foundation, and a research grant from Irving and Cherna Moskowitz.

*ori.grossman@weizmann.ac.il
†erez.berg@weizmann.ac.il

[1] J. A. Hertz, Phys. Rev. B **14**, 1165 (1976).
[2] T. Moriya, *Spin Fluctuations in Itinerant Electron Magnetism* (Springer, New York, 1985).
[3] A. J. Millis, Phys. Rev. B **48**, 7183 (1993).
[4] D. Belitz, T. R. Kirkpatrick, and T. Vojta, Rev. Mod. Phys. **77**, 579 (2005).
[5] H. V. Löhneysen, A. Rosch, M. Vojta, and P. Wölfle, Rev. Mod. Phys. **79**, 1015 (2007).
[6] C. Nayak and F. Wilczek, Nucl. Phys. **B417**, 359 (1994).
[7] C. M. Varma, Z. Nussinov, and W. van Saarloos, Phys. Rep. **361**, 267 (2002).
[8] T. Senthil, Phys. Rev. B **78**, 035103 (2008).
[9] J. Polchinski, Nucl. Phys. **B422**, 617 (1994).
[10] Y. B. Kim, A. Furusaki, X.-G. Wen, and P. A. Lee, Phys. Rev. B **50**, 17917 (1994).
[11] V. Oganesyan, S. A. Kivelson, and E. Fradkin, Phys. Rev. B **64**, 195109 (2001).
[12] W. Metzner, D. Rohe, and S. Andergassen, Phys. Rev. Lett. **91**, 066402 (2003).
[13] A. Abanov, A. V. Chubukov, and J. Schmalian, Adv. Phys. **52**, 119 (2003).
[14] A. Abanov and A. Chubukov, Phys. Rev. Lett. **93**, 255702 (2004).
[15] L. Dell'Anna and W. Metzner, Phys. Rev. B **73**, 045127 (2006).
[16] S.-S. Lee, Phys. Rev. B **80**, 165102 (2009).
[17] M. A. Metlitski and S. Sachdev, Phys. Rev. B **82**, 075127 (2010).
[18] E.-A. Kim, M. J. Lawler, P. Oreto, S. Sachdev, E. Fradkin, and S. A. Kivelson, Phys. Rev. B **77**, 184514 (2008).
[19] D. F. Mross, J. McGreevy, H. Liu, and T. Senthil, Phys. Rev. B **82**, 045121 (2010).
[20] D. Dalidovich and S.-S. Lee, Phys. Rev. B **88**, 245106 (2013).
[21] A. L. Fitzpatrick, S. Kachru, J. Kaplan, and S. Raghu, Phys. Rev. B **88**, 125116 (2013).
[22] M. A. Metlitski, D. F. Mross, S. Sachdev, and T. Senthil, Phys. Rev. B **91**, 115111 (2015).
[23] T. Holder and W. Metzner, Phys. Rev. B **92**, 041112(R) (2015).
[24] C. M. Varma, Phys. Rev. Lett. **115**, 186405 (2015).
[25] P. Lunts, A. Schlief, and S.-S. Lee, Phys. Rev. B **95**, 245109 (2017).
[26] The $d = 2$ problem can be controlled in certain especially designed limits of either a large number of fermion flavors, long-range interactions with an exponent close to a certain critical value, or both [6,19,27,28]. However, it remains unclear how these limits connect to the physical limit of a finite number of flavors and finite-range interactions.
[27] J. A. Damia, S. Kachru, S. Raghu, and G. Torroba, Phys. Rev. Lett. **123**, 096402 (2019).
[28] P. Säterskog, B. Meszena, and K. Schalm, Phys. Rev. B **96**, 155125 (2017).
[29] A. Abanov, A. V. Chubukov, and A. Finkel'stein, Europhys. Lett. **54**, 488 (2001).
[30] S. Lederer, Y. Schattner, E. Berg, and S. A. Kivelson, Phys. Rev. Lett. **114**, 097001 (2015).
[31] H. Löhneysen, M. Sieck, O. Stockert, and M. Waffenschmidt, Physica (Amsterdam) **223B–224B**, 471 (1996).
[32] A. Rost, S. A. Grigera, J. Bruin, R. Perry, D. Tian, S. Raghu, S. A. Kivelson, and A. Mackenzie, Proc. Natl. Acad. Sci. U.S.A. **108**, 16549 (2011).
[33] C. M. Moir, S. C. Riggs, J. A. Galvis, X. Lian, P. Giraldo-Gallo, J.-H. Chu, P. Walmsley, I. R. Fisher, A. Shekhter, and G. S. Boebinger, npj Quantum Mater. **4**, 8 (2019).
[34] B. Michon, C. Girod, S. Badoux, J. Kačmarčík, Q. Ma, M. Dragomir, H. A. Dabkowska, B. D. Gaulin, J. S. Zhou, S. Pyon, T. Takayama, H. Takagi, S. Verret, N. Doiron-Leyraud, C. Marcenat, L. Taillefer, and T. Klein, Nature (London) **567**, 218 (2019).
[35] P. Walmsley, C. Putzke, L. Malone, I. Guillamón, D. Vignolles, C. Proust, S. Badoux, A. I. Coldea, M. D. Watson, S. Kasahara, Y. Mizukami, T. Shibauchi, Y. Matsuda, and A. Carrington, Phys. Rev. Lett. **110**, 257002 (2013).
[36] B. Ramshaw, S. Sebastian, R. McDonald, J. Day, B. Tan, Z. Zhu, J. Betts, R. Liang, D. Bonn, W. Hardy *et al.*, Science **348**, 317 (2015).
[37] B. I. Halperin, P. A. Lee, and N. Read, Phys. Rev. B **47**, 7312 (1993).

[38] E. Berg, M. A. Metlitski, and S. Sachdev, Science **338**, 1606 (2012).
[39] Y. Schattner, M. H. Gerlach, S. Trebst, and E. Berg, Phys. Rev. Lett. **117**, 097002 (2016).
[40] Y. Schattner, S. Lederer, S. A. Kivelson, and E. Berg, Phys. Rev. X **6**, 031028 (2016).
[41] Z.-X. Li, F. Wang, H. Yao, and D.-H. Lee, Sci. Bull., **61**, 925 (2016).
[42] M. H. Gerlach, Y. Schattner, E. Berg, and S. Trebst, Phys. Rev. B **95**, 035124 (2017).
[43] X. Wang, Y. Schattner, E. Berg, and R. M. Fernandes, Phys. Rev. B **95**, 174520 (2017).
[44] X. Y. Xu, K. Sun, Y. Schattner, E. Berg, and Z. Y. Meng, Phys. Rev. X **7**, 031058 (2017).
[45] Z.-X. Li, F. Wang, H. Yao, and D.-H. Lee, Phys. Rev. B **95**, 214505 (2017).
[46] S. Gazit, M. Randeria, and A. Vishwanath, Nat. Phys. **13**, 484 (2017).
[47] X. Wang, Y. Wang, Y. Schattner, E. Berg, and R. M. Fernandes, Phys. Rev. Lett. **120**, 247002 (2018).
[48] Z. H. Liu, G. Pan, X. Y. Xu, K. Sun, and Z. Y. Meng, Proc. Natl. Acad. Sci. U.S.A. **116**, 16760 (2019).
[49] C. Bauer, Y. Schattner, S. Trebst, and E. Berg, Phys. Rev. Research **2**, 023008 (2020).
[50] E. Berg, S. Lederer, Y. Schattner, and S. Trebst, Annu. Rev. Condens. Matter Phys. **10**, 63 (2019).
[51] S. Lederer, Y. Schattner, E. Berg, and S. A. Kivelson, Proc. Natl. Acad. Sci. U.S.A. **114**, 4905 (2017).
[52] M. Bercx, F. Goth, J. S. Hofmann, and F. F. Assaad, SciPost Phys. **3**, 013 (2017).
[53] R. Blankenbecler, D. J. Scalapino, and R. L. Sugar, Phys. Rev. D **24**, 2278 (1981).
[54] F. Assaad and H. Evertz, in *Computational Many-Particle Physics*, Lecture Notes in Physics Vol. 739, edited by H. Fehske, R. Schneider, and A. Weiße (Springer, Berlin Heidelberg, 2008), pp. 277–356.
[55] U. Wolff, Phys. Rev. Lett. **62**, 361 (1989).
[56] F. F. Assaad, Phys. Rev. B **65**, 115104 (2002).
[57] See Supplemental Material at http://link.aps.org/supplemental/10.1103/PhysRevLett.127.017601 for more details, where we elucidate how the specific heat was extracted from the DQMC data and discuss finite size scaling, provide details of the calculation within RPA approximation, and discuss the crossovers in the electron Green's function upon approaching the QCP, including Refs. [58–61].
[58] A. Moreo and D. J. Scalapino, Phys. Rev. Lett. **66**, 946 (1991).
[59] N. Trivedi and M. Randeria, Phys. Rev. Lett. **75**, 312 (1995).
[60] F. Marsiglio and J. P. Carbotte, Electron-phonon superconductivity, in *Superconductivity: Conventional and Unconventional Superconductors*, edited by K. H. Bennemann and J. B. Ketterson (Springer Berlin Heidelberg, Berlin, Heidelberg, 2008) pp. 73–162.
[61] Y. Wang, A. Abanov, B. L. Altshuler, E. A. Yuzbashyan, and A. V. Chubukov, Phys. Rev. Lett. **117**, 157001 (2016).
[62] Note that this is the specific heat at a fixed chemical potential, rather than at a fixed density.
[63] In this temperature regime, the direct contribution of the bosonic degrees of freedom appears to be small, presumably since these are gapless only close to $q = 0$ (as opposed to the fermionic degrees of freedom which are gapless over the entire Fermi surface.).
[64] We note that, strictly speaking, there is no notion of a gap at finite T, due to the presence of thermal excitations.
[65] Here, for simplicity, we assume Z and m^* to be direction independent.
[66] T. Holder and W. Metzner, Phys. Rev. B **90**, 161106(R) (2014).
[67] Y. Wu, A. Abanov, Y. Wang, and A. V. Chubukov, Phys. Rev. B **102**, 024525 (2020).
[68] A. Klein, A. V. Chubukov, Y. Schattner, and E. Berg, Phys. Rev. X **10**, 031053 (2020).
[69] L. Dell'Anna and W. Metzner, Phys. Rev. Lett. **98**, 136402 (2007).
[70] D. L. Maslov, V. I. Yudson, and A. V. Chubukov, Phys. Rev. Lett. **106**, 106403 (2011).
[71] X. Wang and E. Berg, Phys. Rev. B **99**, 235136 (2019).
[72] S. Licciardello, J. Buhot, J. Lu, J. Ayres, S. Kasahara, Y. Matsuda, T. Shibauchi, and N. Hussey, Nature (London) **567**, 213 (2019).
[73] W. K. Huang, S. Hosoi, M. Čulo, S. Kasahara, Y. Sato, K. Matsuura, Y. Mizukami, M. Berben, N. E. Hussey, H. Kontani, T. Shibauchi, and Y. Matsuda, Phys. Rev. Research **2**, 033367 (2020).
[74] M. Bristow, P. Reiss, A. A. Haghighirad, Z. Zajicek, S. J. Singh, T. Wolf, D. Graf, W. Knafo, A. McCollam, and A. I. Coldea, Phys. Rev. Research **2**, 013309 (2020).
[75] A. I. Coldea, S. F. Blake, S. Kasahara, A. A. Haghighirad, M. D. Watson, W. Knafo, E. S. Choi, A. McCollam, P. Reiss, T. Yamashita *et al.*, npj Quantum Mater. **4**, 2 (2019).
[76] https://alf.physik.uni-wuerzburg.de.